

## ASPECTS REGARDING INTERLAMINAR STRESS DISTRIBUTION ON THE COMPOSITE LAMINATED SKIN OF A TAIL ROTOR BLADE EXPOSED TO AERODYNAMIC FORCES

Andrei - Daniel VOICU\*<sup>1</sup>, Anton HADĂR<sup>2</sup>, Daniel VLĂSCEANU<sup>3</sup>

**Rezumat.** Realizarea unui structurii compozite performante trebuie să țină seamă de o multitudine de factori care influențează răspunsul structurii la solicitările apărute pe timpul exploataării. Astfel, în cazul învelișului laminat al unei pale compozite anticuplu, proiectată pentru a înlocui pala metalică a elicopterului IAR330, este important să se analizeze distribuția de tensiuni pe fiecare lamină constituantă, astfel încât, soluția constructivă aleasă să fie optimă. Modulul ACP Post din cadrul programului Ansys Workbench oferă posibilitatea vizualizării acestei caracteristici ulterior analizei statice structurale a palei, precum și a valorii coeficienților de siguranță în funcție de criteriul de rupere utilizat.

**Abstract.** *In realizing a high-performance composite material, it is important to take into consideration all the factors that influence the structural response of the component when exposed to service conditions. Thus, in the case of the laminar skin of a composite tail rotor blade, the study of the stress distribution on each lamina is important, so that the optimal design can be chosen. The ACP Post module of the Ansys Workbench finite element software offers the possibility of visualizing the stress distribution on each lamina of the skin, as well as the value of the safety factor for multiple failure criteria.*

**Keywords:** helicopter tail rotor blade, laminar composite materials, failure criteria.

### 1. Introduction

Since their development, composite materials have been viewed as superior materials which have the capability of enhancing the overall performances of the structures that contained them. They have been used for decades in their simpler forms in various industries such as constructions, where concrete has been a significant strengthening composite material.

Advanced composite materials on the other hand are still the subject of various research domains, due to their high strength fibers which exhibit a low density while occupying a large fraction of the volume [1]. Specific advantages such as

<sup>1</sup> P.h.D. Student, University Politehnica of Bucharest, 313 Splaiul Independenței, Sector 6, Bucharest, Romania (email: [voicu\\_andrei2001@yahoo.com](mailto:voicu_andrei2001@yahoo.com) / [voicu@roaf.ro](mailto:voicu@roaf.ro)).

<sup>2</sup> Prof., P.h.D., Department of Strength of Materials, University Politehnica of Bucharest, 313 Splaiul Independenței, Sector 6, Bucharest, Romania, Member of the Romanian Academy of Scientists (e-mail: [anton.hadar@upb.ro](mailto:anton.hadar@upb.ro)).

<sup>3</sup> Associate professor, P.h.D., Department of Strength of Materials, University Politehnica of Bucharest, 313 Splaiul Independenței, Sector 6, Bucharest, Romania (e-mail: [daniel.vlasceanu@upb.ro](mailto:daniel.vlasceanu@upb.ro)).

increased strength, reduced mass and design flexibility make them a key candidate for replacing metal structures in the aerospace industry.

Nowadays, advanced composite materials fabrication represents a multibillion-dollar market and some of the main promoters for the development of new advanced composite materials are generally large companies who can afford the development of new technological procedures and large-scale manufacturing, such as:

- N.A.S.A. - for program such as the Advanced Space Transportation Program [2];
- U.S.A.F. - lightweight armor protection for the military aviation and also structural components;
- commercial companies that provide materials for aerospace manufacturers, such as: Cytec Solvay, Hexcel, SGL, TenCate and Teijin [3].

Making the transition from conventional metal alloys to advanced composite materials represents an important step in increasing the overall performances of any aircraft, especially if the progression towards a helicopter with modern structural components is not opportune in the near future, due to financial factors.

Such is the case of the IAR330 military transport helicopter, currently on active duty with the Romanian Air Force, which is equipped with five aluminum alloy tail rotor blades as can be seen in figure 1.



**Fig. 1.** In flight view of the IAR330 military transport helicopter [4]

The current article presents certain results regarding the research done with the purpose of obtaining a reliable and enhanced composite tail rotor blade, with respect to interlaminar stress distribution and factor of safety.

---

Rouchon was among the first to introduce the concept of pyramid of tests with regard to certification of aircraft composite structures [5], thus presenting a methodology towards realizing a reliable composite structure.

A similar certification procedure was presented by Bruyneel et al. [6], while making a parallel approach between numerical analysis simulations and physical tests required to validate them, as can be seen in figure 2.

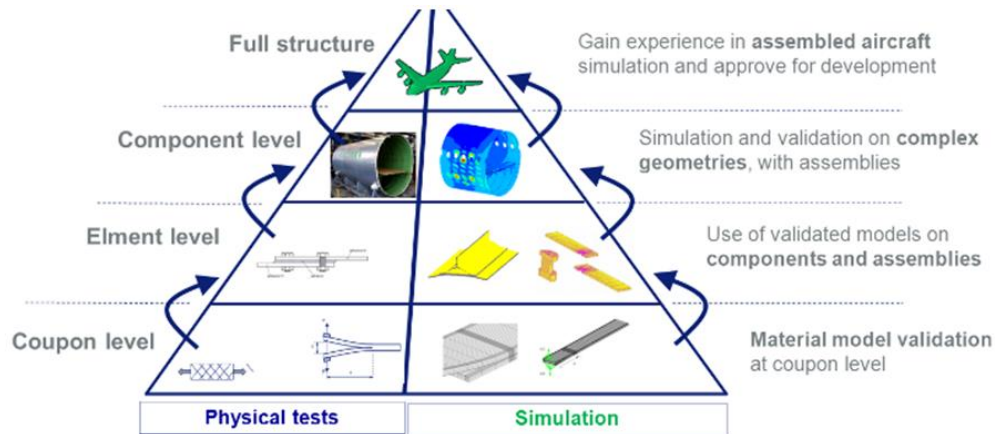


**Fig. 2.** The pyramid of tests, divided into physical and virtual testing at each stage [6]

Some of the manufacturers involved in designing advanced composites work accordingly with the U.S.A.F. military standard MIL-HDBK-17-1-E in order to be accepted as a supplier by the corresponding aviation authorities [7].

## 2. Interlaminar stress distribution in the skin of the blade

The theory of laminated plates assumes that there are no interlaminar stress components due to the planar nature of the multidirectional laminate and could be used for structures without discontinuities, such as free edges. The stress distribution in the vicinity of the free edge of a boundary layer is three-dimensional. The boundary layer is a region of the laminate where the stress transfer between the plies is realized through the action of laminar stresses [8].

The damage initiation process at the free edge of a composite laminate is influenced by the interlaminar stresses present in the boundary layer along the free edge. The main result of the action of interlaminar stresses is the delamination between layers.

According to J.C. Halpin [8], interlaminar stresses appear in laminated composite materials due to mismatch in engineering properties between the plies. His study of composite laminates indicates that for a laminated composite with fibers orientated at  $0^\circ$ ,  $90^\circ$ ,  $+45^\circ$ ,  $-45^\circ$ , the interlaminar shear stresses will be significantly lower if the  $+45^\circ$  and  $-45^\circ$  plies are separated by a  $0^\circ$  or  $90^\circ$  ply.

Interlaminar stresses by definition are either normal to the plane of the laminate ( $\sigma_3 / \sigma_z$ ) or are defined as shear stresses along the edges of the laminate ( $\tau_{23}$  and  $\tau_{13} / \tau_{yz}$  and  $\tau_{xz}$ ), as can be seen in figure 3.

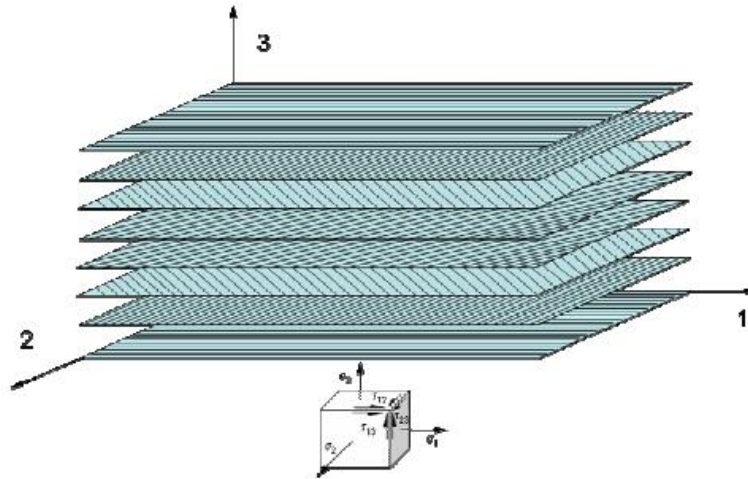


**Fig. 3.** View of the interlaminar stress components [9]

In order for a reduction of the interlaminar stress values to occur, one of the two following measures must be taken:

- an appropriate stacking sequence of the laminas must be realized;
- a reduction of the concentrated plies with the same orientation.

The final laminated composite must have uniformly dispersed plies throughout the entire thickness, an advantage being the symmetry of the laminate about the mid plane [9]. Also, the flexural axis ply imbalance can be reduced thru the use of angled plies ( $\pm 45^\circ$ ).

The fiber orientation and ply distribution for the laminated composite skin of the blade can be observed in figure 4.

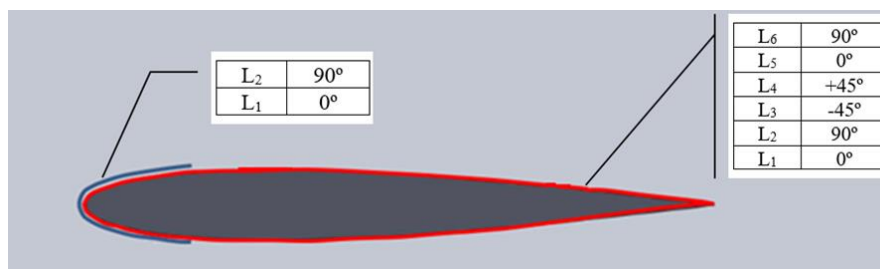


**Fig. 4.** Ply distribution over the PVC foam core of the blade

The skin of the blade consists of six prepreg carbon fiber epoxy resin laminates, with the following orientation:  $0^\circ / 90^\circ / -45^\circ / +45^\circ / 0^\circ / 90^\circ$ . With an approximated thickness of 0.25 mm for each lamina, the total skin thickness is about 1.5 mm. The material properties of the composite used to fabricate the skin are presented in table 1.

**Table 1.** Material properties of the skin of the blade

Material property	Value
Young modulus on x direction - $E_x$ (MPa)	61340
Young modulus on y direction - $E_y$ (MPa)	61340
Young modulus on z direction - $E_z$ (MPa)	6900
Poisson's ratio in xy plane - $\nu_{xy}$	0.04
Poisson's ratio in yz plane - $\nu_{yz}$	0.3
Poisson's ratio in xz plane - $\nu_{xz}$	0.3
Shear modulus in xy plane - $G_{xy}$ (MPa)	19500
Shear modulus in yz plane - $G_{yz}$ (MPa)	2700
Shear modulus in xz plane - $G_{xz}$ (MPa)	2700

The composite blade is filled with a polymeric PVC foam which is suitable for sandwich structures in aerospace application, and has a density of  $80 \text{ kg/m}^3$  and Young's modulus of approximately 102 MPa.

The blade has been loaded with the aerodynamic pressures obtained from the fluid flow analysis, which have been previously validated by placing the blade in a subsonic wind tunnel [10].

The stress distribution on the outer and inner faces of each of the six laminas can be observed in figures 5-12.

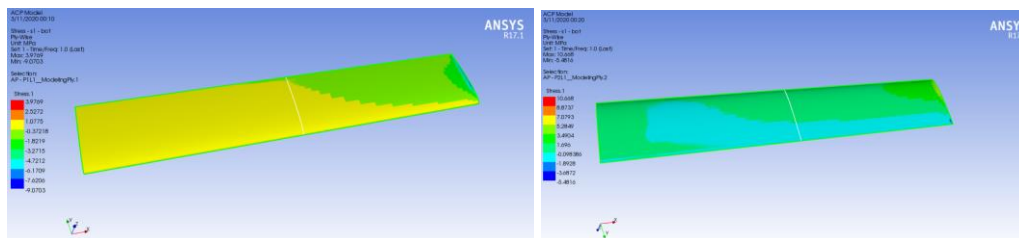


**Fig. 5.** Stress distribution on the first lamina - Outer (left) and inner (right) surfaces

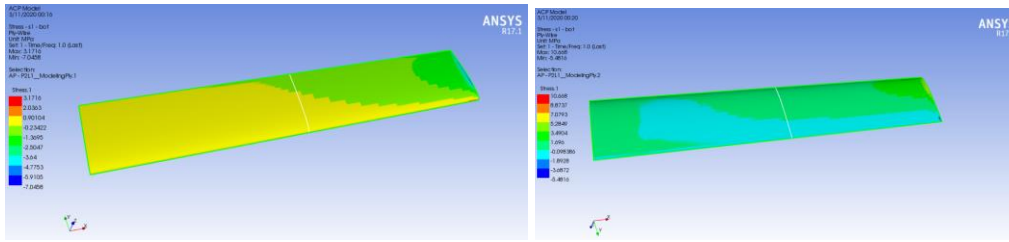


Fig. 6. Stress distribution on the second lamina - Outer (left) and inner (right) surfaces

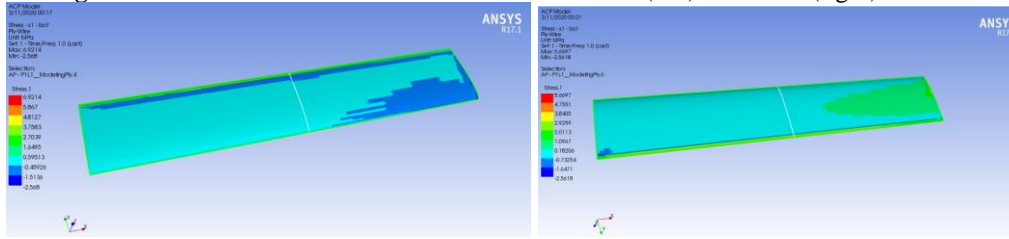


Fig. 7. Stress distribution on the third lamina - Outer (left) and inner (right) surfaces

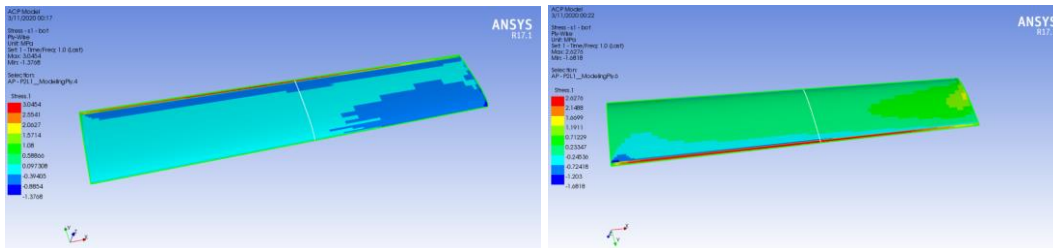


Fig. 8. Stress distribution on the fourth lamina - Outer (left) and inner (right) surfaces

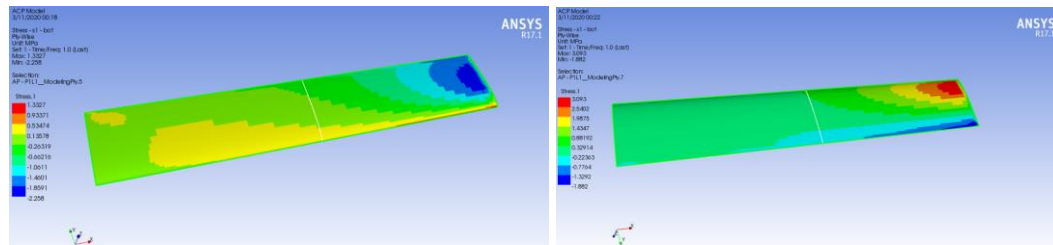


Fig. 9. Stress distribution on the fifth lamina - Outer (left) and inner (right) surfaces

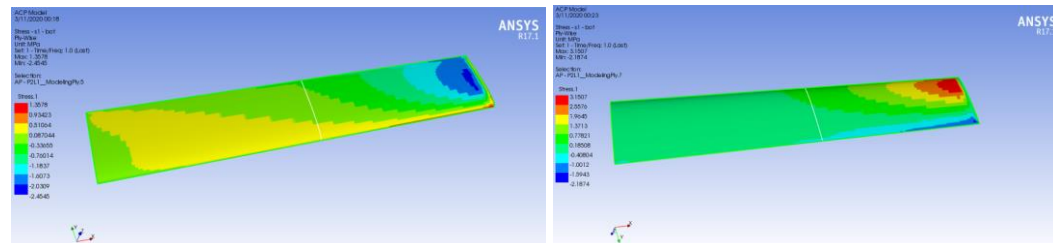
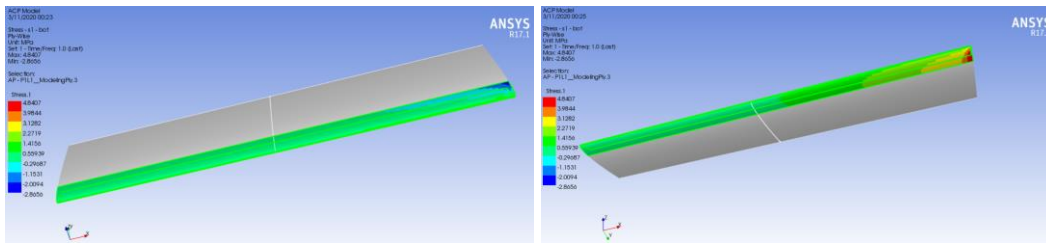
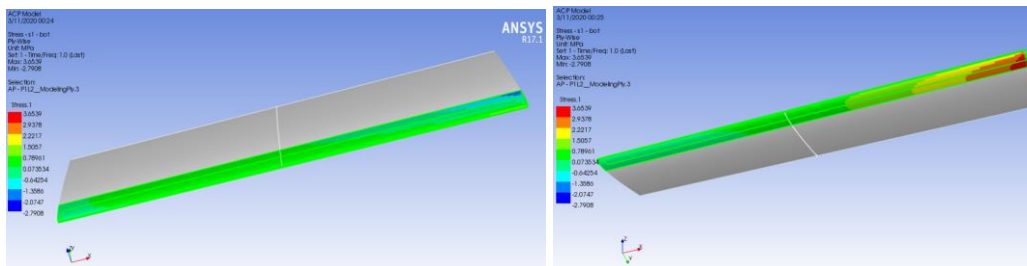


Fig. 10. Stress distribution on the sixth lamina - Outer (left) and inner (right) surfaces





**Fig. 11.** Stress distribution on the first lamina of the leading-edge reinforcement - Outer (left) and inner (right) surfaces



**Fig. 12.** Stress distribution on the second lamina of the leading-edge reinforcement - Outer (left) and inner (right) surfaces

As it was expected, the maximum stress is localized at the foot of the blade where a fixed support is placed and due to the high pressure values on the exterior surfaces, the free end of the blade is bending in the direction of the air flow, resulting in a tensile load on the outer laminas and compression on the inner laminas, as it can be seen from the previous figures.

The maximum stress is exhibited on the first lamina of the composite skin, with a value of 13.854 MPa which is well below the modulus of elasticity presented previously. The maximum stress on the leading edge protection is 4.8407 MPa, localized also around the fixed end of the blade.

### 3. Safety factor assessment using different failure criterions

The study of composite failure modes is a complex process based on the orthotropic nature of these material types. There are currently no equations that can link the failure modes, loading conditions, material properties and the level of stress/strain. The main objective of all the current research done in the structural failure analysis domain is orientated towards finding a criterion that can be universally accepted by designers and engineers. The currently existing failure criterions can be divided in two categories: those dependent on failure modes and those which are not dependent on failure modes [11].

Some of the main modes in which failure can occur are the following:

- Composite failure when exposed to tension - manifested as fiber rupture due to high loads on the fiber direction or as matrix cracking, due to stress concentrations located around the fiber or high shear stress on the fiber direction;
- Composite failure when exposed to compression:
  - Compressive loads on the direction of the fibers leads to fiber breakage or micro-buckling;
  - Compression in the transversal plane of the fiber direction may lead to matrix / fiber cracking or delamination.
- Composite failure due to shear forces - develops as a result of stress concentrators located on the fibers or in the matrix.

Composite failure is characterized by an initial elastic phase, when damage is not present in the structure, followed by a phase in which stress levels induce the appearance of material damage and a later post-failure phase, when damage propagates inside the structure [12, 13].

Damages affecting multi-layered composite laminates can be classified in two main categories and can occur either separately or simultaneously [12, 13, 14]:

- Intra-laminar failures - such as fiber rupture and debonding between fiber and matrix;
- Inter-laminar failures - such as delamination, that appear at the interface between two adjacent plies.

Due to the anisotropic nature which characterizes composite materials and the difference in the material properties of the components, a general failure theory which can be applied to all available designs and scenarios does not exist. Therefore, in order to establish the safety factor of composite structure, there have been developed multiple failure theories, some of which are integrated in finite element programs.

Some of the main criterions used nowadays to study the failure modes of a composite blade are:

- ❖ *Tsai-Wu* - is a material failure theory which is widely used for anisotropic composite materials that possess different strengths when exposed to tension and compression. Failure occurs when the failure index in a laminate reaches 1. The criterion can be expressed in the following mathematical form [15]:

$$F_i \cdot \sigma_i + F_{ij} \cdot \sigma_i \cdot \sigma_j \leq 1 \quad (1)$$



where:

-  $i, j = 1 \div 6$ ;

-  $F_i, F_{ij}$  - experimentally determined material strength parameters;

-  $\sigma_i, \sigma_j$  - symmetric tensors expressed in Voigt notation;

- ❖ *Maximum Stress* - failure will occur when the structural stress ( $\sigma_1, \sigma_2, \tau_{12}$ ) is higher than the corresponding yield strength, when exposed to tension or compression; this criterion is a linear, stress based and failure mode dependent criterion without stress interaction (resulting in five subcriteria and five failure mechanisms) [16]. The following conditions must be satisfied in order for the material to resist the applied loads (tensile, compression and shear):

$$\sigma_1 < X_t \quad (2)$$

$$\sigma_2 < Y_t \quad (3)$$

$$\sigma_1 > X_c \quad (4)$$

$$\sigma_2 > Y_c \quad (5)$$

$$|\tau_{12}| < S \quad (6)$$

- ❖ *Maximum Strain* - failure appears when one of the strain directional components is exceeded, by comparing the manifested strain with experimentally determined uniaxial strains at failure. It is similar to the maximum stress failure criterion, with the major difference being that the strains are limited instead of stresses. Failure occurs when one or more of the following inequalities is not satisfied [17]:

$$\varepsilon_1 < X_{\varepsilon_t} \quad (7)$$

$$\varepsilon_2 < Y_{\varepsilon_t} \quad (8)$$

$$|\gamma_{12}| < S_{\varepsilon} \quad (9)$$

$$\varepsilon_1 < X_{\varepsilon_c} \quad (10)$$

$$\varepsilon_2 < Y_{\varepsilon_c} \quad (11)$$

where:

-  $X_{\varepsilon_t} (X_{\varepsilon_c})$  - is the maximum tensile (compressive) normal strain in the 1-direction;

- $Y_{\varepsilon_t}$  ( $Y_{\varepsilon_c}$ ) - is the maximum tensile (compressive) normal strain in the 1-direction;
- $S_{\varepsilon}$  - the maximum shear strain in the 1-2 coordinate system.

The previous two equations are available for composite materials which possess different strengths in terms of tension and compression.

- ❖ *Tsai-Hill* - is a phenomenological material failure theory used to predict failure of a composite when the failure index in a laminate reaches 1. This criterion takes into account the interaction between stresses, not being able to identify the failure mode. Ply failure appears when the following condition is satisfied [18]:

$$\left(\frac{\sigma_{11}}{X_{11}}\right)^2 - \left(\frac{\sigma_{11} \cdot \sigma_{22}}{X_{11}^2}\right) + \left(\frac{\sigma_{22}}{X_{22}}\right)^2 + \left(\frac{\sigma_{12}}{X_{12}}\right)^2 \leq 1 \quad (12)$$

where:

- $X_{11}$  is the maximum strength of the ply in the longitudinal direction;
- $X_{22}$  is the maximum strength of the ply in the transversal direction;
- $X_{12}$  is the in-plane shear maximum strength of the ply between the longitudinal and the transversal directions.
- ❖ *Puck* - is a realistic 3D fracture criterion based on experimental observations that takes into consideration the heterogeneous structure of the material which is relevant to the failure mode. Specific differences between fiber fracture and inter-fiber fracture have been highlighted and also a fracture angle parameter has been introduced to characterize the fracture in the plane parallel to the fibers [12]. The failure criterion for fiber fracture in a fixed plane perpendicular to the fiber orientation is described by the following relationship:

$$\left(\frac{\sigma_1}{R_{\parallel}^{t,c}}\right)^2 = 1 \quad (13)$$

where:

- $R_{\parallel}^t$  - is the longitudinal strength for  $\sigma_1 > 0$ ;
  - $R_{\parallel}^c$  - is the longitudinal strength for  $\sigma_1 < 0$ ;
-

The corresponding relationship that describes the inter-fiber failure embodies a natural coordinate system and a fracture angle which are utilized to describe the material stress and also the fracture direction. It has the following form:

$$\max_{\theta} f(\sigma_n, \tau_{nt}, \tau_{n1}) = 1 \quad (14)$$

- ❖ *Cuntze* - is an invariant based composite failure criterion, which can be adjusted to study the failure of unidirectional, bi-directional and multi-layered composites, by changing the fracture calculation mode for each individual failure type. This criterion is based on the results obtained from a multitude of experimental tests presented by the author in his article [5]. The five independent failure modes for unidirectional composites (two fiber failures and three inter-fiber failures) can be characterized by the following relationships [14]:

$$I_1 = \sigma_1 \quad (15)$$

$$I_2 = \sigma_2 + \sigma_3 \quad (16)$$

$$I_3 = \tau_{31}^2 + \tau_{21}^2 \quad (17)$$

$$I_4 = (\sigma_2 - \sigma_3)^2 + 4 \cdot \tau_{23}^2 \quad (18)$$

$$I_5 = (\sigma_2 - \sigma_3)(\tau_{31}^2 - \tau_{21}^2) + 4 \cdot \tau_{23} \cdot \tau_{32} \cdot \tau_{21} \quad (19)$$

- ❖ *LaRC* - is a phenomenological failure criterion developed by N.A.S.A.'s Langley Research Center, that takes into consideration the "in situ" effect of composite materials. The LaRC02, LaRC03 and LaRC04 theories utilize a series of criteria that are based on experimental observations, fracture mechanics and micromechanical modeling. The capabilities of these criteria are as follows [19]:

- *LaRC02* - is based a physically based criterion based on Hashin's unidirectional laminates criteria and the action plane concept developed by Puck. It has the capability of predicting matrix and fiber failures, without requiring curve-fitting parameters;
- *LaRC03* - utilizes six different equations to predict the matrix and fiber failure without curve-fitting parameters, with the angle of fracture plane being found by thru Mohr-Coulomb hypothesis for matrix failure under compression in the transverse plane;

- *LaRC04* - is a modified version of the LARC03 criterion which has the capability of predicting three dimensional tensions and in-plane shear non-linearity.

A numerical analysis for a composite version of the tail rotor blade which equips the IAR330 helicopter has been realized in order to asses which failure criterion is the most restrictive in terms of margin of safety. The blade was exposed to predetermined fluid flow aerodynamic pressures, similar to the conditions existing during flight. The ACP Post module of the Ansys Workbench software offers the possibility of determining the safety factor for each ply of a multi-layered composite material, such as the skin of the tail rotor blade. Figure 14 depicts the skin of the composite blade and the fiber orientation directions.

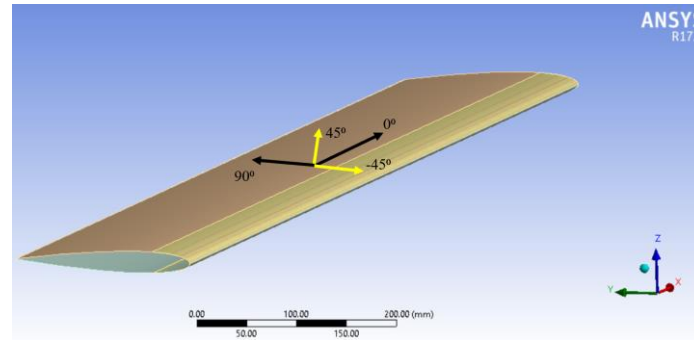


**Fig. 14.** Fiber orientation direction for the skin of the composite tail rotor blade

The general formula for determining the safety factor of the structure is:

$$c = \frac{\sigma_{\text{lim}}}{\sigma_a} \quad (20)$$

In table 2 the safety factor values for each of the six plies of the composite are presented, by using the following failure criterions: Hasin, Cruntze and Tsai-Wu.

**Table 2.** The safety factor values for the six plies of the composite skin

<i>Ply number</i>	<i>Safety factor</i>		
	<i>Hasin</i>	<i>Cruntze</i>	<i>Tsai-Wu</i>
1	34.567	10.921	42.588
2	46.718	13.477	59.135
3	58.373	31.546	59.748
4	45.78	33.499	47.714
5	31.672	17.894	31.672
6	26,742	13.618	26.742

From the previous presented results, it can be concluded that the skin of the blade can withstand with ease the pressures created by the moving airflow in flight. Judging by the results, Cruntze is the most restrictive of the three safety factors previously presented, while Tsai-Wu is the most permissive.

### **Conclusions**

Interlaminar stress study is an important topic needed to be studied in order to assess the structural resistance of a laminated composite material. The ACP Pre and ACP Post modules available in Ansys Workbench are powerful and useful tools which can be used to determine stress values and obtain a visual distribution of them on each individual lamina.

Evaluating the structural integrity can be achieved with multiple failure criteria (Maximum strain, Maximum stress, Tsai-Hill, Tsai-Wu, etc.), the most efficient of them being available in most modern numerical analysis software. The benefit of using them is the rapid localization of possible failure or stress concentrators which can lead to future fractures.

The composite laminated skin of the IAR330 tail rotor blade is subjected to aerodynamic pressures in order to evaluate the mechanical response of the structure. From the previously presented results, the structure handles the load efficiently, making it suitable for realizing a practical model for validation. Further research shall be done regarding the ply distribution and orientation, in order to obtain a structure with high performances.

### **Acknowledgment**

This work is supported by the project ANTREPRENORDOC, in the framework of Human Resources Development Operational Programme 2014-2020, financed from the European Social Fund under the contract number 36355/23.05.2019 HRD OP /380/6/13 - SMIS Code: 123847.

## **R E F E R E N C E S**

- [1] [https://en.wikipedia.org/wiki/Advanced\\_composite\\_materials\\_\(engineering\)](https://en.wikipedia.org/wiki/Advanced_composite_materials_(engineering))
  - [2] [https://en.wikipedia.org/wiki/NASA\\_Advanced\\_Space\\_Transportation\\_Program](https://en.wikipedia.org/wiki/NASA_Advanced_Space_Transportation_Program)
  - [3] <https://www.businesswire.com/news/home/20160926005678/en/Top-5-Vendors-Global-Advanced-Composites-Market>
  - [4] [https://ro.wikipedia.org/wiki/IAR\\_330](https://ro.wikipedia.org/wiki/IAR_330)
-

- [5] J. Rouchon, *Certification of large aircraft composite structures, recent progress and new trends in compliance philosophy* (17th ICAS, Stockholm, Sweden, 1990).
- [6] M. Bruyneela, J.P. Delsemmea, A.C. Goupila, *Damage modeling of laminated composites: validation of the inter-laminar law of SAMCEF at the coupon level for UD plies*, (ECCM16 - 16TH European conference on composite materials, Seville, Spain, 22-26 June 2014).
- [7] Handbook - Polymer matrix composites, MIL-HDBK-17-1E, 23 January 1997
- [8] J. C. Halpin, *Primer on Composite Materials Analysis* (CRC Press, 1992).
- [9] <https://www.compositesaustralia.com.au/wp-content/uploads/2011/12/Designing-with-Composite-Materials-Part-7F-%E2%80%93-Detail-Design-%E2%80%93-Interlaminar-Stresses.pdf>
- [10] A.D. Voicu, A. Hadăr, D. Vlăsceanu, *Validation of a numerical fluid flow analysis for a helicopter tail rotor blade using a subsonic wind tunnel*, (Macromolecular Symposia, 2020) vol. **389** (1).
- [11] A. De Luca, F. Caputo, *A review on analytical failure criteria for composite materials* (AIMS Materials Science Journal, 2017), vol. **4** (5), pp.1165-1185.
- [12] A. Puck, *Festigkeitsanalyse von Faser-Matrix-Laminaten: Modelle für die Praxis* (224 Seiten, Carl Hanser Verlag, München, Wien, 1996).
- [13] R. G. Cuntze, A. Freund, *The predictive capability of failure mode concept-based strength criteria for multidirectional laminates* (Composite Science and Technology, 2004), vol. **64**, pp. 343-377.
- [14] R. M. Grothaus, *Analysis of composite failure behaviour based on size effect invariant failure criterion* (EAST-4D Carbon Technology GmbH, Hauboldstr. 8, 01239 Dresden, Germany)
- [15] S. W. Tsai, E. M. Wu, *A general theory of strength for anisotropic materials* (Journal of Composite Materials, 1971), vol. **5**, pp. 58-80.
- [16] Ng LinFeng, S. DharMalingam, S. Irulappasamy, *Failure Analysis in Biocomposites, Fibre-Reinforced Composites and Hybrid Composites* (Woodhead Publishing Series in Composites Science and Engineering, 2019), pp. 79-95.
- [17] R. M. Jones, *Mechanics of composite materials* (CRC Press, 1998).
- [18] M. C. Niu, *Composite Airframe Structures* (Conmilit Press LTD, Hong Kong, 2010).
-

- [19] S. T. Pinho, C. G. Dávila, P. P. Camanho, L. Iannucci, P. Robinson, *Failure Models and Criteria for FRP Under In-Plane or Three-Dimensional Stress States Including Shear Non-Linearity*, (National Aeronautics and Space Administration, 2005), NASA/TM-2005-213530.
-